J. Cosmet. Sci., 69, 257–267 (July/August 2018)

Stability Studies and Characterization of Glutathione-Loaded Nanoemulsion

NAVEED ULLAH KHAN, ATIF ALI, HIRA KHAN, ZAHEER ULLAH KHAN, and ZIA AHMED, *Department of Pharmaceutics, College of Pharmaceutical Sciences, Soochow University, Suzhou 215123, P. R. China (N.U.K.), Department of Pharmacy, COMSATS University Islamabad, Abbottabad Campus, Abbottabad 22060, Pakistan (A.A., Z.U.K.), Department of Pharmaceutical Sciences, Abbottabad University of Science and Technology, Havelian, Abbottabad 22500, Pakistan (H.K., Z.A.)*

Accepted for publication July 6, 2018.

Synopsis

Glutathione reduced (GSH) is the mother of all the antioxidants and has an antimelanogenic effect. It is extremely vulnerable to oxidation in the solution form which limits its use. The GSH in nano-oil droplets present a potential solution to this problem. The aim of this study was to formulate glutathione-loaded nanoemulsion and assess its stability studies over a 90-day testing period. To formulate GSH-loaded nanoemulsion pseudo-ternary phase diagram, it was built with various concentrations of water, liquid paraffin oil, and surfactant mixture (Tween 80 and Span 80). The oily phase was prepared by dissolving the GSH (450 mg) in liquid paraffin oil through stirring. High-energy homogenization was used to prepare the nanoemulsion. From preformulation stability studies of the 28-day testing period, nanoemulsion (NE-19) with oil and surfactant mixture ratio (1:1) of hydrophilic lipophilic balance (HLB) value 10 was selected. The samples of NE-19 and its respective base (B-19) were kept at four different storage conditions for a period of 90 days and evaluated for physical characteristics, droplet size and distribution analysis, zeta potential analysis, electrical conductivity, mobility, polydispersity, pH, phase separation, and flow analysis at different time intervals. Glutathione in nano-oil droplets with nonionic surfactants produced oil-in-water nanoemulsions that were thermodynamically stable over the 90-day testing period at different storage conditions. NE-19 was formulated having non-Newtonian flow and pseudo-plastic behavior. pH was found in the range of 5–6. Polydispersity was less than 0.3. The droplet size of fresh nanoemulsion was 96.05 nm, whereas the zeta potential was −37.1. Mobility and electrical conductivity were −2.726 μm cm/Vs and 0.0141 mS/cm, respectively. Glutathione-loaded nanoemulsions have excellent stability, promising the solution in nano-oil droplets and are suggested for *in-vivo* release studies for oxidative skin related diseases.

INTRODUCTION

In contemporary eras, extensive and continuous development in consumer claim in the field of cosmetics has spurred the development of sophisticated formulations, aiming at high performance, attractive appearance, sensorial benefit, and safety. Although with increasing

Address all correspondence to Atif Ali at ajmaline2000@gmail.com or atifali@ciit.net.pk.

demand from consumers, the formulators have certain problems regarding the optimum equilibrium between active compound concentration and the formulation base for skin structure regarding the ideal penetration of the active compound into the natural skin barrier (1).

Glutathione is a resilient antioxidant often called the mother of all the antioxidants. It is a tripeptide antioxidant based on three amino acids; cysteine, glycine, and glutamine (2,3). Glutathione transpires in both reduced (GSH) and oxidized (GSSG) states. The GSH is a biologically active sulfhydryl group which allows for interactions with a variety of biochemical systems. It is the most crucial molecule needed to stay healthy and prevents diseases. Apart from its several natural purposes, it is thought to be a contributory in generating skin lightening because of its tyrosinase-inhibitory activity (2).

Many lightening compounds are melanocyte-toxic (2). These melanocyte-toxic compounds are oxidized in the cell to harvest extremely deleterious intermediates such as quinones. These quinones retract melanocytes, ultimately triggering spanking of pigment. But GSH is purported to shield the melanocytes from oxidation through its antioxidant protective effects (4,5). GSH is extremely exposed to oxidation in the solution form. GSH is hydrolyzed by intestinal and hepatic gamma-glutamyl transferase, resulting in abridged bioavailability when directed orally. Most of the absorbed GSH sustains within the gut luminal cells and could be found in the general circulation (6). So, it produces pronounced stability and absorption complications (7) which restrain their persistence for new formulations. The submicron or nano-size of active molecules is enough to cross the skin barriers during penetration into the skin (8,9). The drug molecules sized in nanometer range offer some exclusive features which can lead to sustained circulation, upgraded drug localization, enhanced drug efficacy, *etc.*, and by means of the variety of dosage forms these better performances can be accomplished. Chemically unstable drugs can be supplied to the skin by means of nanosystems (10). A nanoemulsion can resolve these issues because it has the ability to protect GSH as the GSH will be in the oil globule of a O/W nanoemulsion. It has been shown that the smaller the particle size the greater the absorption into skin *Stratum corneum* (1). The *S. corneum* is the first-line barrier of the skin because of its lipophilicity and high cohesion between cells (11). Hence, good stability and penetration efficacy could be attained. That is why a GSH-loaded nanoemulsion was formulated to achieve the desired stability.

MATERIALS AND METHODS

MATERIALS

Glutathione reduced 98% (GSH) was purchased from Acros organics (Fair Lawn, NJ). Liquid paraffin oil was purchased from Merck (KGaA, Darmstadt, Germany). Polyethylene glycol sorbitan monooleate (Tween 80) and sorbitan monooleate (Span 80) were purchased from Merck. All other chemicals were of analytical grades.

METHODS

A modified method was adopted to prepare the GSH-loaded nanoemulsion (1). Surfactant mixture (S_{mix}) was dissolved in distilled water with continuous agitation to prepare a

homogeneous aqueous phase. Oily phase was prepared by the dissolving GSH in liquid paraffin oil through stirring. The oil phase was added to the aqueous phase drop-by-drop with constant stirring by a magnetic stirrer at the rate of 1,100 rpm (12). The homogenized mixture (coarse emulsion) was left stirring for 2 h, at 1,100 rpm at room temperature, and then, it was homogenized with a high-pressure homogenizer at 15,000 rpm for 10 min (13). The concentration of GSH (450 mg) was kept constant by adjusting each formulation (14). The pseudo-ternary phase diagram is very significant in finding the optimum concentrations of the ingredients while preparing a nanoemulsion (15). Different concentrations of liquid paraffin oil, water, and S_{mix} were mixed and nanoemulsion regions were determined (Figure 1) by constructing the pseudo-ternary phase diagram using the software Chemix School 3.60 (Arne Standes, Burgen, Norway).

To develop a stable o/w nanoemulsion, several preliminary stability studies were performed. These nanoemulsions were made from pseudo-ternary phase diagrams having HLB values 9, 10, 11, and 12. The HLB value was kept greater than eight. Three PTPDs (Pseudo Ternary Phase Diagrams) were constructed by keeping constant the oil concentration and S_{mix}. Thirty-three nanoemulsions (w/w) were made in which the HLB values of NE-1 to NE-6, NE-7 to NE-12, NE-19 to NE-23, NE-13 to NE-18, NE-24 to NE-28, and NE-29 to NE-33 were 9, 10, 11, and 12, respectively. These formulations were subjected to preliminary stability studies over a 28-d testing period at 25°C in an incubator. Two nanoemulsions, NE-18 and NE-19 were stable during this preliminary stability study. The nanoemulsions NE-18 and NE-19 were again tested for a 90 days at 25°C to find the most stable nanoemulsion (Table I).

NE-19 was stable, whereas phase separation was found at the end of the 90-d testing period in NE-18. During this preformulation stability study factors such as color, phase separation, and liquefaction were observed. The NE-19 having a HLB value of 10 was selected and eight samples of nanoemulsions (B-19 and NE-19, four samples each) were

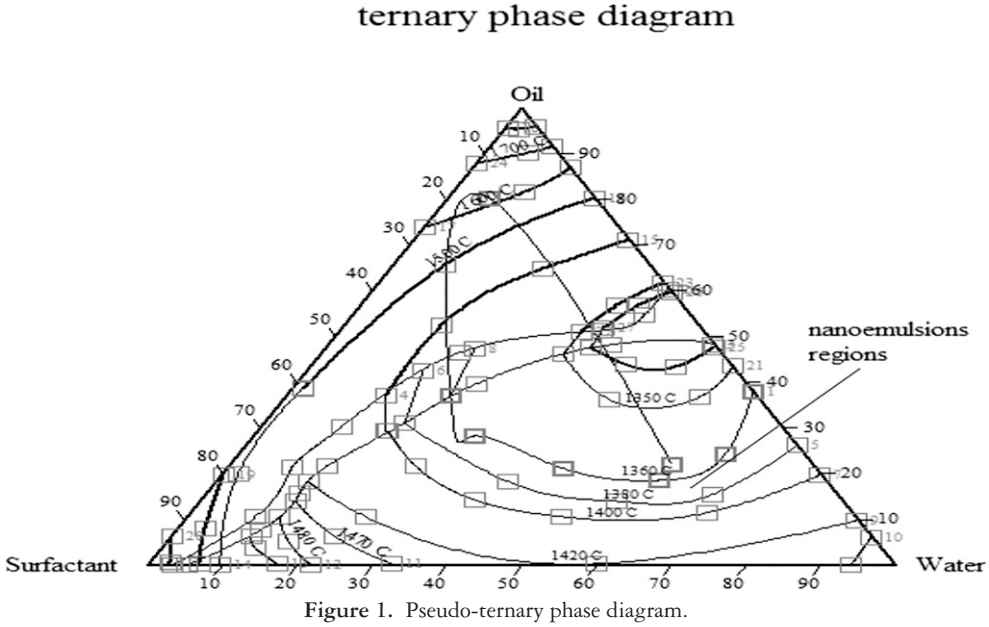

Figure 1. Pseudo-ternary phase diagram.

Table I
Preliminary Stability Study of NE-18 and NE-19 for the 90-d Testing Period

Formulations S/No	Nanoemulsion code	Effects at 25°C, after		
		30 d	60 d	90 d
1	NE-18	Stable	Stable	Phase separation
2	NE-19	Stable	Stable	Stable

repeated and prepared to evaluate the stability studies according to ICH (International Council for Harmonisation) guidelines (16). B-19 was without GSH. Four samples each of B-19 and NE-19 were kept at four different storage conditions which were 4, 25, 40, and 40°C ± 75% RH (Relative humidity) (16) and observed at intervals of 0 h, 24 h, 48 h, 72 h, 7 d, 14 d, 21 d, 28 d, 45 d, 60 d, and 90 d. Color, odor, and liquefaction of B-19 and NE-19 were clarified by means of visual appearance (17). The pH measurements were taken by means of a pH meter (model Zubehorbox pH; InoLab, Weilheim, Germany). Phase separation analysis was performed by centrifugation of B-19 and NE-19 at 5,000 rpm for 10 min in a centrifugation machine (model: 5810R; Eppendorf, Hamburg, Germany). The turbidity of NE-19 and B-19 was noted visually.

Flow characteristics were measured with a cone-plate rheometer, using CP41 spindle and operated with the software Rheocalc 1.01 (Brookfield Digital Rheometer, Model DV-III, Brookfield Engineering Laboratories, Middleborough, MA). The viscosities of fresh NE-19 and B-19 were measured at 100–200 rpm speed (with 50 increments). All the measurements ($n = 3$) were taken at 25°C on a rheometer For evaluation of flow characteristics (16), Power's Law was applied as follows:

$$\tau = kD^n,$$

where, τ = shear stress, D = yield stress (stress at zero shear rate), k = plastic viscosity, and n = shear rate.

Analysis of the average diameter is very significant for the confirmation of nanoemulsion droplet size. The NE-19 was evaluated for mean droplet size, zeta potential, mobility, electrical conductivity, and polydispersity by using dynamic light scattering (Zetasizer, model ZS; Malvern Instruments, Worcestershire, UK). Measurements were performed at 25°C using a scattering angle of 90° (10). The average droplet size, zeta potential, mobility, electrical conductivity, and polydispersity were recorded for samples of NE-19 (0 d, 30 d, 60 d, and 90 d).

STATISTICAL ANALYSIS

Statistical analysis was performed using SPSS software by applying two-way ANOVA (Analysis of variance) (16).

RESULTS

The two nanoemulsions NE-18 and NE-19 were stable after the 28-d testing period, whereas other formulations showed instability at different time intervals (Table I), which

were subjected further to a 90-d testing period. The results showed that NE-19 was the most stable formulation for the fabrication of GSH stability. NE-18 showed phase separation at the end of the testing period. Freshly prepared B-19 and NE-19 were milky white, had pleasant odor, and had no phase separation after accelerated centrifugation test at the start of the testing period and remained stable at the end of the 90-d period (Figure 2). No phase separation was found in samples of B-19 and NE-19 kept at 4 and 25°C after each subsequent time interval, but at 90 d, phase separation was observed in samples of B-19 and NE-19 kept 40 and 40°C ± 75 RH. There was no turbidity seen. The pH values measured at various storage conditions are shown in Table II. The average droplet size and zeta potential, mobility, and electrical conductivity of freshly prepared B-19 recorded were 184.25 nm, −30.85 mV, −2.911 μm cm/Vs, 0.254, and 0.0236 mS/cm, respectively. The average droplet size and zeta potential, mobility, polydispersity, and electrical conductivity of NE-19 recorded are shown in Table III. The droplet size distribution and intensity distribution of NE-19 are shown in Figure 3.

The Power's law math model provided the analysis of the behavior of data sets. The viscosities of freshly prepared B-19 and NE-19 were found to be 3,363.492 and 4,425.712 cP, respectively. Flow index of B-19 and NE-19 were 0.28 and 0.21, respectively. Confidence of fit of the base and NE-19 were found to be 99.6 and 99.8, respectively. Rheograms for B-19 and NE-19 have been shown in Figure 4.

DISCUSSION

Nanoemulsions are appealing delivery systems because of their high stability, low amount of surfactants, low viscosity, and good development. They are significant because of their small droplet size and close contact with the *S. corneum*, so the active molecules easily reach the site of action (1).

In topical formulations, GSH is at risk of degradation as it oxidizes quickly in water. In GSH-loaded (o/w) nanoemulsion, GSH can be prevented from degradation as it remains inside oil globules dispersed in the aqueous phase. That is why a GSH-loaded o/w nanoemulsion was fabricated to increase the stability of GSH.

The modified method was adopted to fabricate a GSH-loaded nanoemulsion to achieve the smallest globule size because the smaller the droplet size, the more stable the nanoemulsion

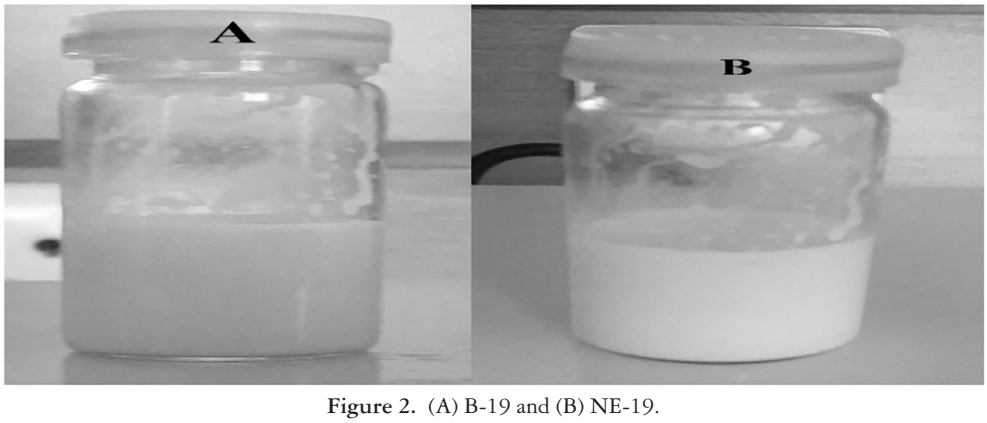

Figure 2. (A) B-19 and (B) NE-19.

Table II
pH Values for B-19 and NE-19 Kept at 4, 25, 40, and 40°C + 75% RH

	4°C		25°C		40°C		40°C + 75% RH	
Storage time	B-19	NE-19	B-19	NE-19	B-19	NE-19	B-19	NE-19
Fresh	5.92	5.79	5.92	5.79	5.92	5.79	5.92	5.79
24 h	5.72	5.53	5.61	5.59	5.64	5.53	5.43	5.49
48 h	5.43	5.39	5.28	5.48	5.35	5.11	4.98	5.38
72 h	5.31	5.28	5.12	5.33	5.21	4.95	4.92	5.24
7 d	5.14	5.16	5.04	5.21	5.09	4.87	4.87	5.09
14 d	4.98	5.03	4.91	4.98	4.93	4.84	4.81	4.92
21 d	4.82	4.92	4.68	4.72	4.82	4.72	4.77	4.81
28 d	4.69	4.78	4.49	4.67	4.71	4.68	4.64	4.73
45 d	4.54	4.76	4.41	4.63	4.63	4.65	4.51	4.69
60 d	4.49	4.61	4.39	4.60	4.54	4.61	4.39	4.67
90 d	4.41	4.53	4.35	4.47	4.48	4.43	4.31	4.37

will be (1,15). Construction of pseudo-ternary phase diagrams is the best way to study all kinds of formulations that can be derived from the mixing of surfactants, water, and oil because the diagrams can cover all probabilities of mixing ratios and possible areas of finding nanoemulsion. All kinds of formulations derived from mixing of oil, water, and surfactants can be studied with the help of a ternary phase diagram for nanoemulsion formulations of liquid paraffin oil, water, and S_{mix} (tween 80 + span 80) with different HLB values 9, 10, 11, and 12. S_{mix} was preferred because a single surfactant was not enough to form the layer at the interface while developing a nanoemulsion. Thirty-three nanoemulsion formulations were derived from pseudo-ternary phase diagrams and subjected to a stability study of 90 days to select the most stable nanoemulsion system. Formulation NE-19 was found to be the most stable formulation having a HLB value of 10. The formulation NE-19 was stable because there was an optimum concentration available to make the interfacial film around the oil globules dispersed in the aqueous phase. This ratio of S_{mix} ($T_{80} = 4.26\%$: $S_{80} = 3.74\%$) increased the interfacial tension of the interfacial film and developed a stable nanoemulsion (18).

Centrifugation involves the application of centripetal force to separate two immiscible liquids and is performed to check whether a nanoemulsion is stable or not. The ability of a formulation to resist change in its physical and chemical characteristics is called its stability (16). NE-19 and B-19 were centrifuged at 5,000 rpm for 10 min. However, no phase separation occurred in the NE-19 and B-19 after centrifugation. The formulations were tested for kinetic stability by centrifugation, and only the formulations that exhibited

Table III
Average Droplet Size and Zeta Potential, Polydispersity, Mobility, and Electrical Conductivity of NE-19 after Different Time Intervals at 25°C

Sample name	Droplet size (nm)	Zeta potential (mV)	Polydispersity index	Mobility (μm cm/Vs)	Electrical conductivity (mS/cm)
Fresh NE-19	96.05	−37.1	0.189	−2.726	0.0141
NE-19 after 30 d	155.0	−34.2	0.208	−2.911	0.0236
NE-19 after 60 d	181.3	−34.8	0.286	−2.684	0.0269
NE-19 after 90 d	190.09	−34.0	0.277	−2.459	0.0289

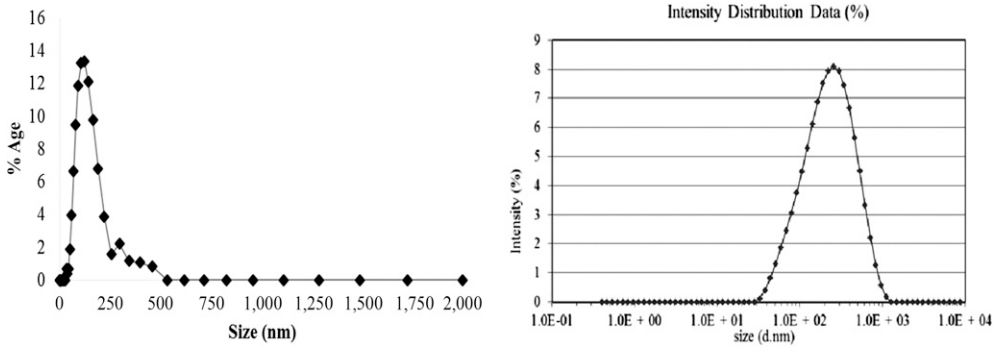

Figure 3. Droplet size distribution and intensity distribution data of freshly prepared NE-19.

no phase separation or inversion, cracking, creaming, or coalescence after these stress tests were selected for further storage stability studies.

Physical characteristics based on visual observations confirm that whether the formulation is physically stable or not (16). The color of the nanoemulsion was milky white, this was because of preparation temperature change, i.e., emulsification at 25°C. With the increase of preparation temperature from 20 to 70°C, the nanoemulsion tends to develop transparency because of the emulsion droplet diameter decreasing from 10.3 μm to 51 nm, proving the formation of nanoemulsions (19). There was no change in the milky white color, no liquefaction, and no phase separation in NE-19 and B-19 on storage at 4, 25, 40, and 40°C + 75% RH over the 90-d testing period. This shows the stability of NE-19. The stability against Ostwald ripening is outstanding because of the extremely low solubility of the paraffin oil in the continuous (19,20), whereas absence of liquefaction provides strong evidence of nanoemulsion stability (21). The absence of liquefaction might be because of the adopted method of high-pressure homogenization. Homogenization decreases liquefaction (22). There was no phase separation in any NE-19 and B-19 samples

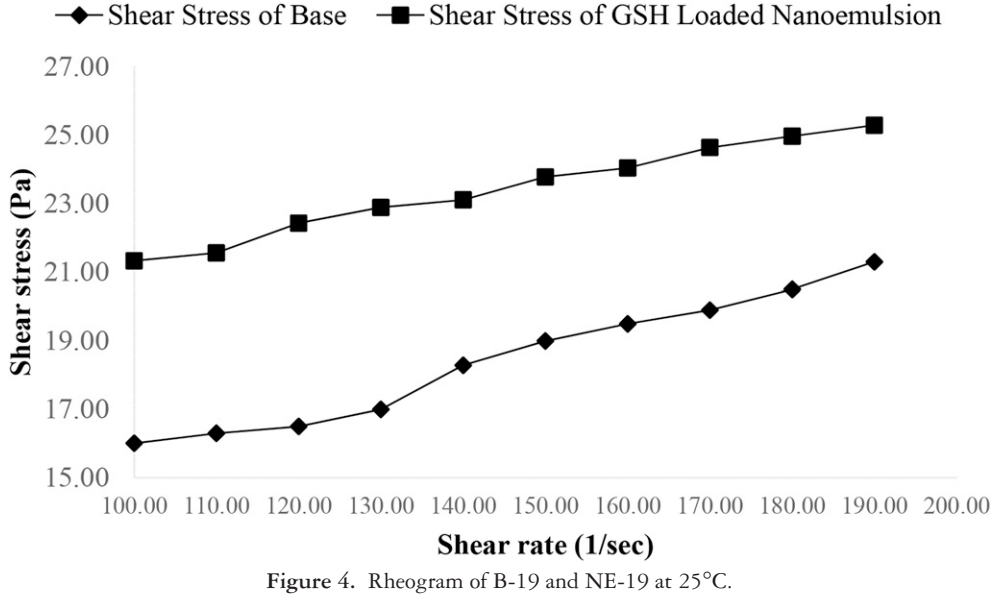

Figure 4. Rheogram of B-19 and NE-19 at 25°C.

at intervals 0 h, 24 h, 48 h, and 72 h, and on days 7, 14, 21, 28, 45, 60, and 90. There was no phase separation in any NE-19 and B-19. However, phase separation occurred in the NE-19 and base stored at 40 and 40°C + 75% RH at the 90th day. This may have occurred because of Ostwald ripening in which molecules move as a monomer, and the formation of larger droplets occurred because of the coalescence of small droplets by diffusion processes driven by the gain in surface free energy (6).

In most colloidal dispersions, the sizes of dispersed structures and the density difference between the continuous and dispersed phase are small enough that thermal energy can keep the colloids from sedimentation under gravity for an extended period of time (21).

Turbidity is haziness or cloudiness or disturbance of a liquid caused by a large number of factors (droplet size, etc.) and the measurement of turbidity is a key test for stability (23). The turbidity of NE-19 and B-19 was checked visually at 4, 25, 40, and 40°C + 75% RH and there was no turbidity seen in them. The variation of the turbidity of a sample as a function of time depends on the flocculation rate. The turbidity of a nanoemulsion results from the contributions of conventional aggregates, bigger drops, and mixed aggregates (24).

pH is the count of total ions present in a formulation. Stable formulations afford very little change in pH. The pH of the skin is normally considered 3–7 (25). The pH of NE-19 tallies with skin pH and there is a little decrease in the pH of NE-19. At the start of the stability study, the pH of fresh samples of NE-19 and B-19 were 5.79 and 5.92. At the end of 90 days of the stability studies, the pH were 4.53, 4.47, 4.43, and 4.37 and 4.41, 4.35, 4.48, and 4.31 at 4, 25, 40, and 40°C + 75% RH, respectively. By applying two-way ANOVA, the change in pH of NE-19 and B-19 was found to be insignificant with respect to time. The pH values of both nanoemulsions, which were unchanged could be because of the stability of the ingredients in the formulation. Thus, this indicated that there was no degradation or ionization of chemicals in the formulation at storage conditions during the testing period. However, because the particle size and the pH value did not significantly change across different conditions, we considered our nanoemulsion to be stable.

Changes in the electrical conductivity can imply nanoemulsion variability and may fluctuate the nanoemulsion droplet size (26). In these studies, the increase in electrical conductivity was minor and prediction of emulsion stability in this way was difficult because the relationship between an increase in electrical conductivity and emulsion instability is not linear. Thus, we could not conclusively determine the nanoemulsion's stability by this parameter. Similar results are reported by Bernardi et al. (27).

Physical stability of nanoemulsions throughout their life is very important, and no or minimal changes in the particle size distribution are necessary. The nanoemulsion stability is strictly related to the nanodroplet size distribution. A large droplet size may enhance Ostwald ripening which causes the increase in droplet size and can lead to creaming and coalescence. A fast droplet size increase indicates low system stability (24). The mean droplet sizes recorded for fresh NE-19, after 30, 60, and 90 days were 96.05 nm, 155, 181.3, and 190, respectively. The range of the droplet size of all formulations should be between 30 and 500 nm (28). There was no large increase in the droplet size of NE-19. The nanoemulsions had polydispersity index values less than 0.3 throughout the 90-d testing period, indicating the high fidelity of the system (low polydispersity), which may reflect the overall stability of this formulation and synthesis method. Polydispersity values near 1.0 are indicative of a polydisperse system (27). The long-term stability of nanoemulsions was evaluated and was also verified by stability studies conducted over 3 mo.

The W/O nanoemulsion produced by high-energy homogenization showed no difference in droplet size over the study period at both 25 and 4°C. The NE-19 demonstrated high physical stability, verifying our results for storage conditions of 4 and 25°C. High-energy homogenization is better at producing stable nanoemulsions than its other preparation methods. When nanoemulsions were prepared using a high-pressure homogenizer, the droplet size was initially around 100 nm; however, the particles increased in size after 30 d at 25°C. This phenomenon was attributed to the preparation method. The high-energy emulsification method used in our study showed high stability with respect to the droplet size and polydispersity index (29).

Zeta potential is a measurement of charge on the nanodroplets; when it is high, nanodroplets repel each other because of similar charges. The zeta potential is very significant in determining the stability of nanoemulsions, all the nanoemulsions which have zeta potential greater than ±30 mV are considered more stable (30). The zeta potential of all NE-19 formulations was found to be negative and more stable as zeta potential is greater than ±30 mV. The zeta potential of fresh NE-19 was −37.1 mV; after 30 days, it was −34.2 mV; and after 60 days, it was −34.8 mV. The mobility of fresh NE-19 was −2.726 µm cm/Vs; after 30 days, it was −2.911; and after 60 days, it was −2.59. When the zeta potential is high (>−30 mV), the nanodroplets repel each other because of similar charges and there is no coalescence and aggregation. The charge on the droplet surface causes the transportation of drug molecules through various physiological barriers (31).

Rheological properties characterize the spreadability features of the nanoemulsion (32). There is a decrease in viscosity as the shear rate and shear stress increases. NE-19 and B-19 have shown non-Newtonian flow and shear-thinning pseudo-plastic behavior on varying shear rates, which occurs in cosmetics (33). The decrease in viscosity may be due to surfactants (span 80 and tween 80), which play an important role in nanoemulsion stability and prevent coalescence and aggregation (34).

CONCLUSION

In this study, a thermodynamically stable nanoemulsion was successfully prepared. The droplet sizes were less than 200 nm with good rheology and stability of GSH. It maintained normal skin pH values throughout the 90-d testing period. The zeta potential of −34 mV, which could impede the coalescence and deposit of the oil nanodroplets, generated the stable nanoemulsion formulation. The nanoemulsion was most stable at room temperature compared with the higher temperature (40°C/75 RH) and could be evaluated for treatment of oxidative skin related diseases.

ACKNOWLEDGMENTS

The authors would like to thank Prof. Dr. Nisar Ur Rehman, Chairman, Department of Pharmacy, COMSATS University Islamabad, Abbottabad Campus, for providing cosmetic laboratory services.

REFERENCES

(1) M. N. Yukuyama, D. D. Ghisleni, T. J. Pinto, and N. A. Bou-Chacra, Nanoemulsion: process selection and application in cosmetics—a review, *Int. J. Cosmet. Sci.*, **38**, 13–24 (2016).

(2) C. D. Villarama and H. I. Maibach, Glutathione as a depigmenting agent: an overview, *Int. J. Cosmet. Sci.*, **27**, 147–153 (2005).
(3) A. Meister and M. E. Anderson, Glutathione, *Annu. Rev. Biochem.*, **52**, 711–760 (1983).
(4) M. I. Rendon and J. I. Gaviria JI. Review of skin-lightening agents. *Dermatol. Surg.*, **31**, 886–889 (2005).
(5) F. Alena, W. Dixon, P. Thomas, and K. Jimbow, Glutathione plays a key role in the depigmenting and melanocytotoxic action of N-acetyl-4-S-cysteaminylphenol in black and yellow hair follicles, *J. Invest. Dermatol.*, **104**, 792–797 (1995).
(6) N. A. Zainol, T. S. Ming, and Y. Darwis, Development and characterization of cinnamon leaf oil nanocream for topical application, *Indian J. Pharm. Sci.*, **77**, 422–433 (2015).
(7) D. Stempak, S. Dallas, J. Klein, R. Bendayan, G. Koren, and S. Baruchel, Glutathione stability in whole blood: effects of various deproteinizing acids, *Ther. Drug. Monit.*, **23**, 542–549 (2001).
(8) F. Shakeel, S. Baboota, A. Ahuja, J. Ali, and S. Shafiq, Skin permeation mechanism of aceclofenac using novel nanoemulsion formulation, *Pharmazie*, **63**, 580–584 (2008).
(9) W. E. Bawarski, E. Chidlowsky, D. J. Bharali, and S. A. Mousa, Emerging nanopharmaceuticals, *Nanomedicine*, **4**, 273–282 (2008).
(10) Z. Hu, M. Liao, Y. Chen, Y. Cai, L. Meng, Y. Liu, N. Lv, Z. Liu, and W. Yuan, A novel preparation method for silicone oil nanoemulsions and its application for coating hair with silicone. *Int. J. Nanomedicine*, **7**, 5719–5724 (2012).
(11) A. Lohani, A. Verma, H. Joshi, N. Yadav, and N. Karki, Nanotechnology-based cosmeceuticals, *ISRN Dermatol.*, **2014**, 1–14 (2014).
(12) A. M. M. Eid, N. A. Elmarzugi, and H. A. El-Enshasy, Preparation and evaluation of olive oil nanoemulsion using sucrose monoester, *Int. J. Pharm. Pharm. Sci.*, **5**, 434–440 (2013).
(13) E. Troncoso, J. M. Aguilera, and D. J. McClements, "Development of nanoemulsions by an emulsification-evaporation technique," in Food Process Engineering in a Changing World: Proceedings of the 11th International Congress on Engineering and Food, May 22–26, 2011, Athens, Greece, 2011, pp. 929–930.
(14) D. B. Harry and S. L. Mayron, Pharmaceutical preparations of glutathione and methods of administration thereof. U.S. Patent No. 6,896,899. 24 May 2005.
(15) M. Sajid, M. Sarfaraz, N. Alam, and M. Raza, Preparation, characterization and stability study of dutasteride loaded nanoemulsion for treatment of benign prostatic hypertrophy, *Iran J. Pharm. Res.*, **13**, 1125–1140 (2014).
(16) A. Ali, N. Akhtar, H. Muhammad, and S. Khan, Assessment of physical stability and antioxidant activity of polysiloxane polyalkyl polyether copolymer-based creams, *J. Chem.*, **2013**, 1–7 (2012).
(17) A. Ali and N. Akhtar, Changes in the characteristics of water-in-oil-based high internal phase emulsion containing Moringa leaves extract at various storage conditions, *Trop. J. Pharm. Res.*, **13**, 677–682 (2014).
(18) N. M. Hadzir, M. Basri, M. Basyaruddin, A. Rahman, A. B. Salleh, R. Noor, Z. Raja, A. Rahman, and H. Basri, Phase behaviour and formation of fatty acid esters nanoemulsions containing piroxicam, *AAPS Pharm. Sci. Tech.*, **14**, 456–463 (2013).
(19) L. Yu, C. Li, J. Xu, J. Hao, and D. Sun, Highly stable concentrated nanoemulsions by the phase inversion composition method at elevated temperature, *Langmuir*, **28**, 14547–14552 (2012).
(20) S. S. Lim, M. Y. Baik, E. A. Decker, L. Henson, L. Michael Popplewell, D. J. McClements, and S. J. Choi, Stabilization of orange oil-in-water emulsions: a new role for ester gum as an Ostwald ripening inhibitor, *Food Chem.*, **128**, 1023–1028 (2011).
(21) T. G. Mason, J. N. Wilking, K. Meleson, C. B. Chang, and S. M. Graves, Nanoemulsions: formation, structure, and physical properties, *J. Phys. Condens. Matter*, **18**, R635–R666 (2006).
(22) C. Qian and D. J. McClements, Formation of nanoemulsions stabilized by model food-grade emulsifiers using high-pressure homogenization: factors affecting particle size, *Food Hydrocoll.*, **25**, 1000–1008 (2011).
(23) K. Rahn-Chique, A. M. Puertas, M. S. Romero-Cano, C. Rojas, and G. Urbina-Villalba, Nanoemulsion stability: experimental evaluation of the flocculation rate from turbidity measurements, *Adv. Colloid. Interface Sci.*, **178**, 1–20 (2012).
(24) K. Rahn-Chique, A. M. Puertas, M. S. Romero-Cano, C. Rojas, and G. Urbina-Villalba, Nanoemulsion stability: experimental evaluation of the flocculation rate from turbidity measurements, *Adv. Colloid. Interface Sci.*, **178**, 1–20 (2012).
(25) A. Ali, N. Akhtar, and F. Chowdhary, Enhancement of human skin facial revitalization by moringa leaf extract cream, *Postep. Dermatologii i Alergol*, **31**, 71–76 (2014).
(26) M. Chiesa, J. Garg, Y. T. Kang, and G. Chen, Thermal conductivity and viscosity of water-in-oil nanoemulsions, *Colloids Surf. A Physicochem. Eng. Asp.*, **326**, 67–72 (2008).

(27) D. S. Bernardi, T. A. Pereira, N. R. Maciel, J. Bortoloto, G. S. Viera, G. C. Oliveira, and P. A. Rocha-Filho, Formation and stability of oil-in-water nanoemulsions containing rice bran oil: *in vitro* and *in vivo* assessments, *J. Nanobiotech.*, **9**, 44 (2011).
(28) R. P. Patel and J. R. Joshi, An overview on nanoemulsion: a novel approach, *Int. J. Pharm. Sci. Res.*, **3**, 4640–4650 (2012).
(29) S. Kotta, A. W. Khan, S. H. Ansari, R. K. Sharma, and J. Ali, Formulation of nanoemulsion: a comparison between phase inversion composition method and high-pressure homogenization method, *Drug Deliv.*, **7544**, 1–12 (2013).
(30) S. Honary and F. Zahir, Effect of zeta potential on the properties of nano-drug delivery systems—a review (Part 1), *Trop. J. Pharm. Res.*, **12**, 255–264 (2013).
(31) E. A. Ostrosky, P. A. Rocha-filho, and L. M. Veríssimo, Production and characterization of cosmetic nanoemulsions containing *Opuntia ficus-indica* (L.) mill extract as moisturizing agent, *Molecules*, **20**, 2492–509 (2015).
(32) L. Goehring and C. Bahr, Interfacial mechanisms in active emulsions, *Soft Matter*, **10**, 7008–7022 (2014).
(33) P. S. Clegg, J. W. Tavacoli, and P. J. Wilde, Soft matter one-step production of multiple emulsions, *Soft Matter*, **12**, 998–1008 (2016).
(34) A. Mandal, A. Bera, K. Ojha, and T. Kumar, Characterization of surfactant stabilized nanoemulsion and its use in enhanced oil recovery. *SPE Int. Oilf. Nanotechnol. Conf.*, **6**, 80–92 (2012).